

Optimized Idronoxil-Loaded Polycaprolactone Nanoparticles for Targeted Liver Cancer Therapy: A Novel Approach in Drug Delivery Systems

Lokeshvar Ravikumar¹, Ramaiyan Velmurugan^{1*}, Vinod Kumar Teriveedhi², Pradeep Vidiyala³, Patibandla Jahnavi⁴, Rajeshwar Vodeti⁵, Selvaraja Elumalai⁶

¹Department of Pharmacology, Saveetha College of Pharmacy, Saveetha Institute of Medical and Technical Sciences (SIMATS), Thandalam, Saveetha Nagar, Chennai 602105, India

²Department of Research & Development, Hikma Pharmaceuticals, USA

³Analytical Chemistry, Elixir Medical Corporation 920 N McCarthy Blvd #100, Milpitas, CA 95035

⁴Department of Pharmaceutics, KVSRR Siddhartha College of Pharmaceutical Sciences, Vijayawada, Andhra Pradesh

⁵Department of Pharmaceutics, School of Pharmacy, Anurag University, Hyderabad, Telangana, 500088

⁶Department of Chemistry, Raffles University, Neemrana, Alwar, Rajasthan 301705, India

Abstract

This study aimed to optimize and characterize Idronoxil-loaded Polycaprolactone nanoparticles as a potential drug delivery system for cancer therapy, focusing on improving particle size, encapsulation efficiency, and stability using a factorial design approach. Nanoparticles were synthesized via the ionic gelation method and optimized based on PCL concentration, polyvinyl alcohol (PVA) concentration, and organic phase volume. Characterization included particle size, zeta potential, encapsulation efficiency, morphology (SEM), FT-IR analysis, *in vitro* drug release, and stability testing. Cytotoxicity was assessed against HepG2 liver cancer cells using the MTT assay. The optimized formulation exhibited a particle size of 97.3 nm, a zeta potential of -6.41 mV, and an encapsulation efficiency of 82.07%, ensuring stability and uniform dispersion. FT-IR confirmed the compatibility of Idronoxil with PCL. *In vitro* drug release studies demonstrated a controlled and sustained release profile driven by diffusion and polymer degradation, enhancing therapeutic potential. Stability testing over 90 days at 40°C±5°C validated the nanoparticles' robustness, with minimal variations in drug content and release profiles. Cytotoxicity studies demonstrated a significant dose-dependent anticancer effect on HepG2 cells, with an IC₅₀ concentration of 19.33 µg/mL, suggesting efficient cellular uptake and potential for therapeutic use. The Idronoxil-loaded PCL nanoparticles showed excellent stability, controlled drug release, and potent anticancer activity, highlighting their potential as an effective drug delivery system for cancer therapy. Future research should focus on *in vivo* studies and clinical validation to establish their efficacy and safety in therapeutic applications.

Keywords: Anticancer, Cytotoxicity, Encapsulation Efficiency, Idronoxil, Liver Cancer Cells, Optimisation, Polycaprolactone Nanoparticles.

Introduction

Liver cancer, a global health burden with high mortality rates, remains a formidable challenge in oncology due to its aggressive

nature and limited treatment options. Traditional therapies, including surgery, chemotherapy, and radiotherapy, are often hampered by systemic toxicity, drug resistance, and suboptimal targeting of cancer cells [1, 2].

Received: 31.12.2024

Accepted: 18.01.2025

Published on: 30.06.2025

*Corresponding Author: velmuruganr.scop@saveetha.com

As a result, there is a pressing need for novel therapeutic strategies that combine efficacy with precision. In this context, nanotechnology has emerged as a transformative approach, enabling the delivery of therapeutic agents in a more targeted and controlled manner [3, 4].

Idronoxil, a potent synthetic flavonoid, has shown significant anticancer potential by modulating key cellular pathways such as apoptosis and proliferation. However, its therapeutic application is limited by poor solubility, bioavailability, and rapid metabolism [5, 6]. To overcome these challenges, polymeric nanoparticles have gained attention as a promising drug delivery platform. Among the various polymers, Polycaprolactone (PCL) stands out for its exceptional biocompatibility, biodegradability, and ability to sustain drug release over extended periods. These characteristics make PCL an ideal candidate for encapsulating hydrophobic drugs like Idronoxil, ensuring prolonged circulation time and enhanced tumor accumulation [7- 9].

This study focuses on the formulation, optimization, and characterization of Idronoxil-loaded PCL nanoparticles tailored for liver cancer therapy. By leveraging the unique properties of PCL, we aimed to develop a nanoparticle system capable of improving the solubility, stability, and therapeutic efficacy of Idronoxil. Through a systematic optimization process, we achieved nanoparticles with desirable physicochemical properties, including controlled size, high drug encapsulation efficiency, and a sustained drug release profile. This innovative approach highlights the potential of PCL-based nanoparticles to revolutionize liver cancer treatment by offering a more effective and patient-friendly therapeutic option.

Material and Methods

The Idronoxil was bought in India from Sigma Aldrich. The initial material utilized was Polycaprolactone from SRL chemicals India with a degree of deacetylation of around 75%.

For the synthesis of the nanoparticles, we utilized sodium tripolyphosphate (TPP, Sigma Aldrich, India), glacial acetic acid (Qualigens), and 95% china made ethanol. Because of its surfactant properties, polyvinyl alcohol (PVA) was used. All reagents were of analytical grade and used without further purification.

Ionic Gelation Approach for the Synthesis of Polymeric Nanoparticles Loaded with Idronoxil

Polycaprolactone (PCL) was stirred overnight in 1% acetic acid to dissolve it completely. The pH of the solution was adjusted to 4.7 by adding sodium hydroxide (2M) solution dropwise under continuous stirring. The resulting PCL solution was filtered using a 0.45 μm membrane filter to remove impurities. Separately, 2% polyvinyl alcohol (PVA) solution was prepared in distilled water and heated to 60°C to ensure complete dissolution. After dissolving the idronoxil in 5 ml of ethanol, 30 ml of the filtered PCL solution was added while being stirred magnetically to ensure even dispersion. The PCL-drug solution was then added dropwise to the PVA solution while maintaining magnetic stirring. Following this, 15 ml of sodium tripolyphosphate (TPP) solution was introduced as a crosslinking agent, and the mixture was stirred at varying rates to facilitate nanoparticle formation. The unencapsulated drug, excess PVA, and dissolved PCL were removed by centrifugation at 12,000 rpm for 20 minutes using a cooled centrifuge. To prepare the resultant nanoparticles for additional study, they were rinsed with distilled water, then freeze-dried, and then placed in a vacuum desiccator [10].

Optimization of Nanoparticles by Box-Behnken Design

An experimental methodology was employed to examine critical process parameters (PCL concentration, (A); PVA concentration, (B); and organic phase (C)) to elucidate the impact of independent variables

on key characteristics of quality (particle size, zeta potential, and entrapment efficacy of Idronoxil). The Design Expert program employed the Box-Behnken design within the response surface methodology (RSM) model, restricting the overall design to 17 runs. Table 1 enumerates the three tiers of independent

variables (+1, 0, and -1) alongside essential process and material parameters that influence the final nanoparticle outcome. Polynomial formulas and 3-D surface plots were employed to evaluate independent variables influencing essential quality aspects.

Table 1. Essential Process Parameters that Affect Many Essential Quality Aspects

	Factor 1	Factor 2	Factor 3	Response 1	Response 2	Response 3
Run	A: PolyCaprolactone (PCL)	B: Surfactant (PVA)	C: Organic Phase	PS	ZP	EE
	%	%	%	nm	mV	%
1	10	0.5	10	639	-4.3	63
2	5.5	0.5	15	327	-7.2	79
3	5.5	0.75	20	539	-13.7	71
4	1	0.5	10	106	-2.9	91
5	1	0.25	15	127	-8.6	91
6	5.5	0.5	15	327	-7.2	79
7	1	0.5	20	92	-12.3	91
8	5.5	0.25	20	334	-7.6	82
9	5.5	0.75	10	467	-3.8	62
10	10	0.75	15	628	-5.2	91
11	5.5	0.5	15	327	-7.2	79
12	5.5	0.5	15	327	-7.2	79
13	1	0.75	15	114	-2.4	99
14	10	0.25	15	428	-4.3	86
15	5.5	0.25	10	580	-8.6	56
16	5.5	0.5	15	327	-7.2	79
17	10	0.5	20	223	-13.7	82

The study's results suggest that the use of the Box-Behnken framework of the response surface methodology (RSM) model will significantly facilitate the production of Idronoxil-loaded PCL nanoparticles.

Characterization of Nanoparticles

Drug Polymer Incompatibility Studies using Fourier Transform Infrared Spectroscopy (Ftir) & Differential Scanning Calorimetric Analysis (Dsc)

The specimens were examined using KBr pellet method and analyzed on a Nicolet 520P FT-IR spectrometer with a 4000 – 500 cm⁻¹ range. The DSC analyses were used to

determine drug's compatibility with excipients. DSC 60, Shimadzu, Japan, was used to analyze pure drug and a 1:1 ratio mixture of drug and excipient. Samples 5 mg was carefully weighed and transferred into an aluminium pan was heated and crimped non-hermetically at a rate of 10°C per minuets in sealed aluminium pans between 25°C and 600.0 °C under nitrogen atmosphere [11].

Morphology Study of Nanoparticle

Scanning electron microscopy (SEM) was used to examine the morphology character of the synthesized nanoparticles (SEM; JEOL JMS-6390 apparatus) [12]. A carbon coating

was applied to the samples to improve electron beam conductivity. Electron beam that passes through into the nanoparticle sample generates a raster of signals gives the information about the sample morphology and other characteristics.

Particle Size & Zeta Potential Analysis

A Nano Particle size analyzer with a maximum output of 4 mW and a measurement accuracy of 0.12 m/Vs was employed to assess the surface charge of aqueous systems, utilizing NIST SRM1980 reference standard material. The Henry equation was employed in the Zeta Potential series to compute the zeta potential following the assessment of the particle surface.

$$UE = 2\varepsilon Zf(ka) / 3\eta.$$

Determination of Encapsulation Efficiency

By determining the number of untrapped drugs, the number of drugs entrapped within the nanoparticles was studied indirectly. As previously stated, the nanoparticle was centrifuged, then supernatant solution containing the free, un-encapsulated drug was collected, diluted by methanol, analyzed by HPLC analysis.

$$\text{Entrapment Efficiency (\%)} = (\text{total drug-free drug}) / \text{total drug} \times 100.$$

Drug Content

Encapsulation efficiency (EE) of Idronoxil nanoparticle (50mg) was dispersed in ethanol, vortexed for 5 min and centrifuged by ultracentrifugation at 20,000rpm at 4°C for 30min. The developed HPLC method 0.1% phosphoric acid: acetonitrile with flow rate, 1mL/min, with C18 reverse phase column and the UV detector set at Idronoxil (247 nm) was used to estimate and validate the free amount of Idronoxil in the supernatant. The following equation is used to calculate DC for prepared nanoparticles:

$$\text{Drug Content (\%)} = (\text{total drug-free drug}) / \text{weight of NPs} \times 100.$$

In Vitro Drug Release

The drugs-loaded nanoparticles (50 mg) were dispersed in 900 ml of phosphate buffer at pH 7.4 with a bath temperature was 37±2°C and a rotation speed of 100 rpm for 24 hours. 1 mL of samples were extracted at intervals of time set in advance (0, 1, 2,3,4,6,8,10 hrs) and replaced with an equal volume of freshly prepared buffer solution at time intervals. The drug concentration was measured using HPLC analysis and calculated using the calibration curve methodology.

Stability Testing

The Idronoxil nanoparticles were placed in borosilicate glass vials and sealed, then stored for 90 days at room temperature (40°C 2°C, % RH±5 % RH). For 30-, 60- and 90-days samples were analyzed for drug release, content uniformity of the drug and any physical changes.

In vitro Cytotoxicity Study (MTT Assay)

The MTT assay was employed to assess in vitro cytotoxicity. The HepG2 cell line was obtained from the National Cell Repository of NCCS (Pune, India) and subsequently cultured in our laboratory for further in vitro tests [13]. The 96-well plates contain Roswell Park Memorial Institute Medium (RPMI) 1640, 10% fetal calf serum (FCS), and are maintained at 5%±0.5 CO₂ and 37°C±0.05. Cells were administered drug-loaded nanoparticles at five distinct concentrations: 6.25 µg/ml, 12.5 µg/ml, 25 µg/ml, 50 µg/ml, and 100 µg/ml. All samples include a DMSO content below 0.1 percent. The MTT reagents were present in all cells and were retained for four hours. The cells produced a vivid blue formazan product in a safety cabinet. Subsequently, it was dissolved in a DMSO solution, and a plate reader was employed to measure the absorbance at 550 nm [14, 15]. The subsequent formula was employed to ascertain the viability percentage:

Sample abs/Control abs multiplied by 100 equals the viability percentage.

Results

Factorial Design

Stable droplets of polycaprolactone (PLC) polymeric solution were generated through the ionic gelation process in both the inner and outer phases, which consisted entirely of water. The organic phase was removed from the solvent mixture during evaporation. The minimum particle size, constrained particle size distributions, and appropriate zeta potential were the factors that facilitated adequate drug loading capacity [16]. This study examines the effects of PCL concentration (%), PVA concentration (%), and organic phase as independent factors on various critical quality metrics, including particle size (nm), zeta potential (mV), and entrapment efficacy of Idronoxil (%). Independent variables were computed for the quadratic models. Substantial

values were identified when the model's variables had p values > 0.05.

Impact of Independent Factors on Idronoxil-Loaded Polycaprolactone Nanoparticles

Particle Size

The following is the quadratic equation created for the response for Idronoxil-PLC-NPs:

$$\text{PARTICLE SIZE (A)} = 327.00 + 184.87A + 34.88B - 75.50C + 53.25AB - 100.50AC + 79.50BC - 108.88A^2 + 106.12B^2 + 46.88C^2.$$

The ANOVA analysis indicates that significant model terms for response A are attributed to the independent variables and their interaction effects, with a p-value of less than 0.0001 (Table 2). Table 3 presents the values of adjusted R², anticipated R², and sequential P-value for the particle size of nanoparticles, zeta potential, and encapsulation efficacy of Idronoxil.

Table 2. ANOVA for a Quadratic Particle Size Model

Source	Sum of Squares	df	Mean Square	F-value	p-value	
Model	5.075E+05	9	56388.76	32.43	< 0.0001	significant
A-PolyCaprolactone	2.734E+05	1	2.734E+05	157.27	< 0.0001	
B-Surfactant (PVA)	9730.13	1	9730.13	5.60	0.0499	
C-Organic Phase	45602.00	1	45602.00	26.23	0.0014	
AB	11342.25	1	11342.25	6.52	0.0379	
AC	40401.00	1	40401.00	23.24	0.0019	
BC	25281.00	1	25281.00	14.54	0.0066	
A ²	49910.59	1	49910.59	28.71	0.0011	
B ²	47421.12	1	47421.12	27.28	0.0012	
C ²	9251.64	1	9251.64	5.32	0.0544	
Residual	12170.25	7	1738.61			
Lack of Fit	12170.25	3	4056.75			
Pure Error	0.0000	4	0.0000			
Cor Total	5.197E+05	16				

Table 3. Summary of Various Quadratic Parameters

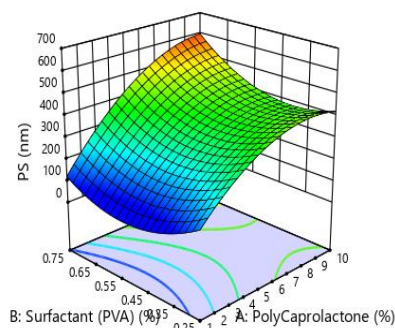
Response	Adjusted R2	Predicted R2	Sequential P-value
Particle size	0.9465	0.6253	0.0009
Zeta potential	0.7573	-0.6988	0.0893
EE	0.8474	-0.0684	0.0010

In the current study, reduced PVA concentration causes nanoparticles to aggregate, grow in size, and become unstable. Nevertheless, elevated PVA concentrations guarantee that the emulsion's external phase exhibits increased viscosity. Consequently, an increased particle size. Consequently, increasing PVA concentrations from 1% to 1.5% has a greater effect on particle size than boosting PVA concentration from 0.5% to 1%. The particle size had been greatly reduced by 1%. The range of the PCL concentration (1 to

3%) had substantial influence on particle size ($p > 0.05$). A rise in PCL concentration could the nanoparticles' particle size should be increased. Because of the greater polymer concentration Poor dispensability into an aqueous solution can be seen during the dispersion phase. Their research shown that particle size increased from 92 nm to 639 nm as Polycaprolactone (PCL) concentration in nanoparticles increased. These are the three-dimensional response graphs of particle size response shown in Figs. 1a, 1b, and 1c illustrate.

PS (nm)

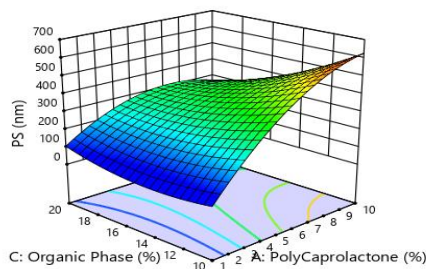
3D Surface



1(A)

PS (nm)

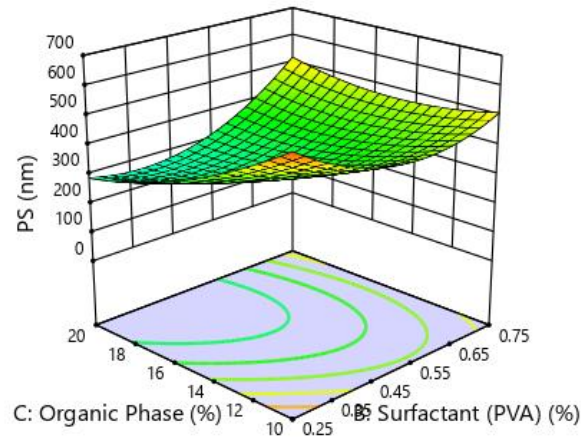
3D Surface



1(B)

PS (nm)

3D Surface



1(C)

Figure 1. Idronoxil-PLC-NPs Three-dimensional Surface Response Plots Illustrating the Impact of (A) Concentration of PCL and Surfactant, (B) Volume of Organic Phase and PCL, (C) Volume of Organic Phase and Concentration of Surfactant

Zeta Potential

The following is the quadratic equation created for the zeta potential response for Idronoxil-PLC-NPs:

$$\text{ZETA POTENTIAL} = -7.20 - 0.1625A + 0.5000B - 3.46C - 1.78AB + 0.0000AC - 2.73BC + 1.0A^2 + 0.9750B^2 - 2.20C^2.$$

The ANOVA analysis results indicate that substantial model terms exist for the response zeta potential, attributed to the independent factors and their interaction effects. The P-value for the response zeta potential was calculated to be 0.0108 (Table 4).

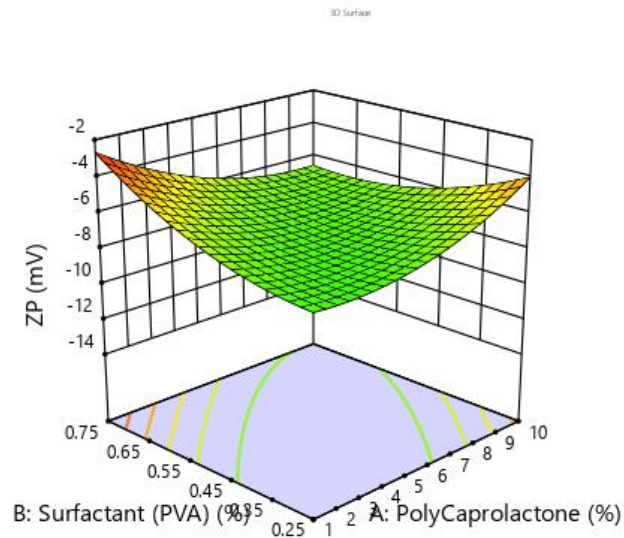
Table 4. Anova for the Model of the Quadratic Zeta Potential

Source	Sum of Squares	Df	Mean Square	F-value	p-value	
Model	168.43	9	18.71	6.55	0.0108	significant
A-PolyCaprolactone	0.2113	1	0.2113	0.0739	0.7936	
B-Surfactant (PVA)	2.00	1	2.00	0.6997	0.4305	
C-Organic Phase	95.91	1	95.91	33.56	0.0007	
AB	12.60	1	12.60	4.41	0.0739	
AC	2.842E-14	1	2.842E-14	9.944E-15	1.0000	
BC	29.70	1	29.70	10.39	0.0146	
A ²	5.09	1	5.09	1.78	0.2236	
B ²	4.00	1	4.00	1.40	0.2753	
C ²	20.38	1	20.38	7.13	0.0320	
Residual	20.01	7	2.86			
Lack of Fit	20.01	3	6.67			
Pure Error	0.0000	4	0.0000			
Cor Total	188.44	16				

A higher negative zeta potential ensures the stability profile of the formulation. An increased PCL concentration may lead to a more negative zeta potential. The situation arises because Polycaprolactone (PCL) is fundamentally an anionic polymer. However, it

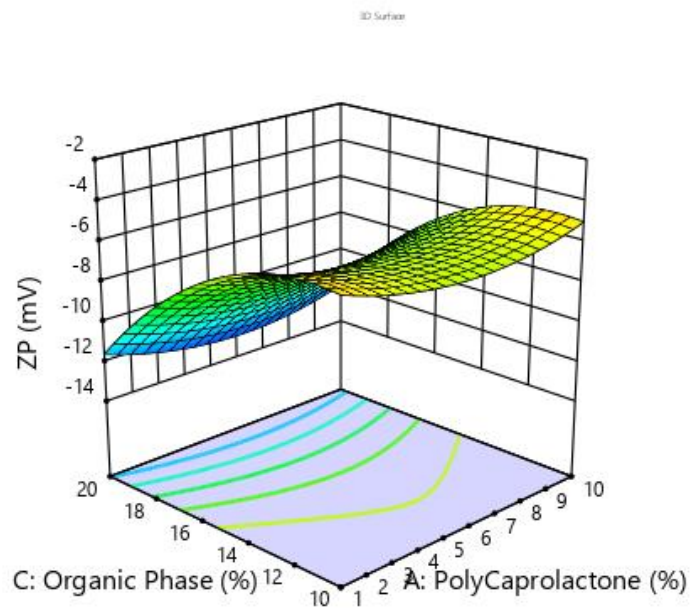
was also acknowledged that increased PVA concentrations elevated negative zeta potential. The zeta potential ranged from -2.4 mV to -13.7 mV. Figures 2a, 2b, and 2c illustrate the three-dimensional response graphs for zeta potential.

ZP (mV)
ZP (mV)



2(A)

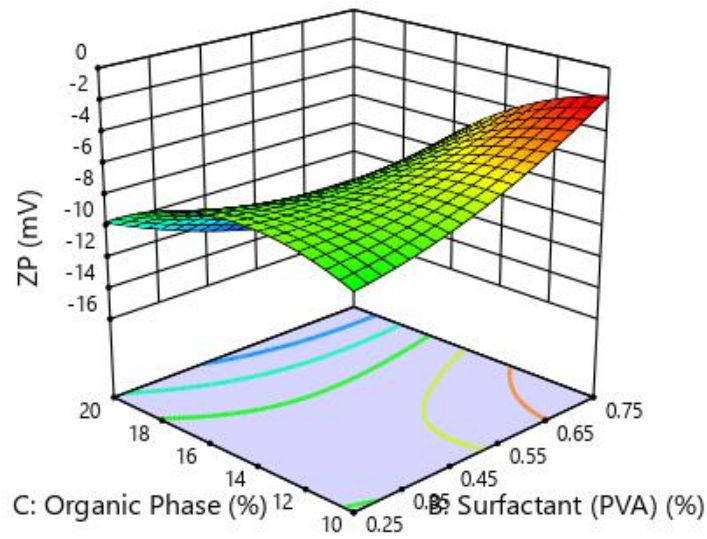
ZP (mV)
ZP (mV)



2(B)

ZP (mV)
ZP (mV)

3D Surface



2(C)

Figure 2. Three-Dimensional Surface Response Plots of Idronoxil-PLC-NPs Illustrating the Influence of (A) Surfactant and PCL Concentration, (B) Organic Volume and PCL, and (C) Organic Phase Volume and Surfactant Concentration.

Encapsulation Efficacy

The following is the quadratic equation created for the response for Idronoxil-PLC-NPs:

$$\begin{aligned} \text{ENCAPSULATION EFFICACY OF} \\ \text{Idronoxil} = & 79.00 - 6.25A + 1.00B + 6.75C - \\ & 0.7500AB + 4.75AC - 4.25BC + 13.37A^2 - \\ & 0.6250B^2 - 10.62C^2. \end{aligned}$$

The ANOVA analysis results indicate significant model terms for the response based on the independent variables and their interaction effects. The P-value for the efficacy of response encapsulation of Idronoxil was established at 0.0020 (Table 5).

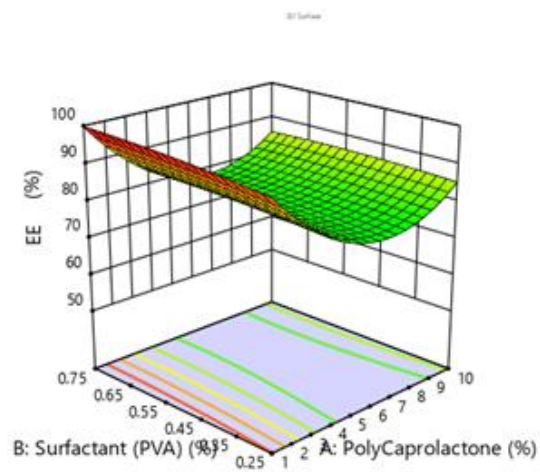
Table 5. Anova for a Quadratic Model of Idronoxil Encapsulation Effectiveness

Source	Sum of Squares	Df	Mean Square	F-value	p-value	
Model	2019.50	9	224.39	10.87	0.0024	significant
A- PolyCaprolactone	312.50	1	312.50	15.14	0.0060	
B-Surfactant (PVA)	8.00	1	8.00	0.3875	0.5533	
C-Organic Phase	364.50	1	364.50	17.66	0.0040	
AB	2.25	1	2.25	0.1090	0.7510	
AC	90.25	1	90.25	4.37	0.0749	
BC	72.25	1	72.25	3.50	0.1036	
A ²	753.22	1	753.22	36.49	0.0005	
B ²	1.64	1	1.64	0.0797	0.7859	
C ²	475.33	1	475.33	23.03	0.0020	

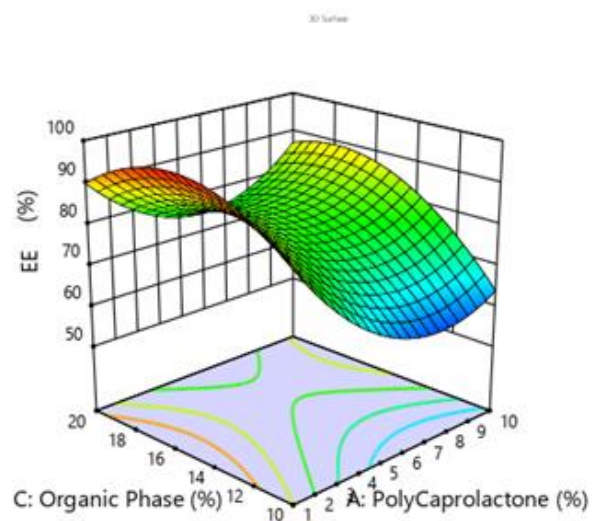
Residual	144.50	7	20.64			
Lack of Fit	144.50	3	48.17			
Pure Error	0.0000	4	0.0000			
Cor Total	2164.00	16				

In this investigation, increasing the concentrations of PVA and PCL would increase the effectiveness of encapsulation. The formulation's encapsulation effectiveness

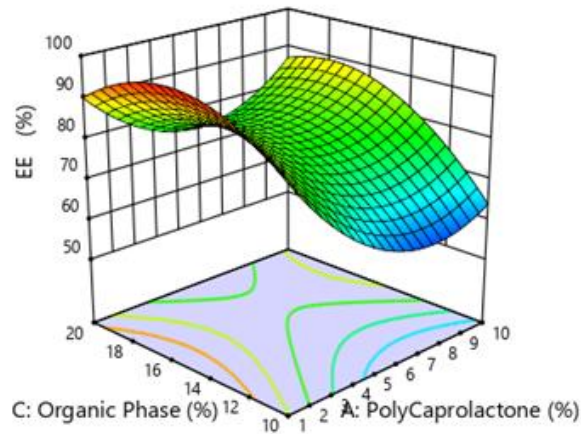
declines as PVA and PLC concentrations are higher. Figs. 3a, 3b, and 3c illustrate the three-dimensional response graphs of EE of Idronoxil.



3(A)



3(B)



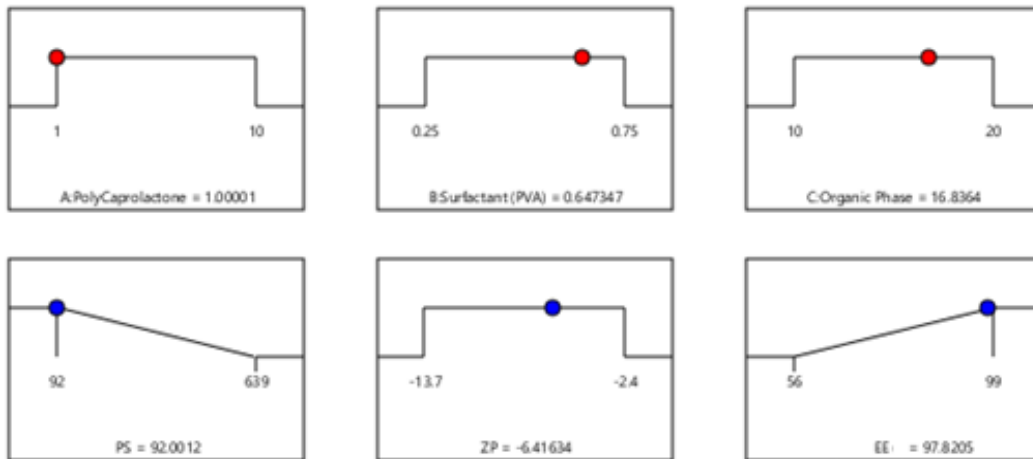
3(C)

Figure 3. Three-Dimensional Surface Response Plots of Idronoxil-PLC-NPs Illustrating the Influence of (A) Surfactant and PCL Concentration, (B) Organic Phase Volume and PCL, and (C) Organic Phase Volume and Surfactant Concentration.

Determination of Optimal Formulation

Figure 4 illustrates the specified ranges for each response, including both input and outcome variables. The overall aesthetic appeal of the design was assessed at 0.939. Optimal nanoparticles should exhibit minimal particle

size, enhanced encapsulation, and elevated anionic zeta potential. The design was established using permselective standards. The connection the optimized batch, actual responses, and anticipated values were shown in Table 6.



Desirability = 0.939
Solution 1 out of 39

Figure 4. Process Optimisation by Desirability Approach.

Table 6. Experimental and Predicted Value of Idronoxil Loaded PCL Nanoparticles

Input variables	Response variables	Experimental values	Predicted values
PLC concentration (%)	Particle size(nm)	97.3	92.002
PVA concentration (%)	Zeta potential(mV)	-6.41	-6.41634
Organic phase (%)	Encapsulation efficacy of Idronoxil (%)	97.8	97.8205

Drug Polymer Incompatibility Studies

FT-IR Spectroscopy

The interaction between Idronoxil, and Polymeric was investigated using Fourier transform Infrared Spectroscopy and the KBr disc method. FT-IR spectrophotometer has been used to capture spectra for Idronoxil, PCL, and a physical mixture of Idronoxil and the polymers PCL in a 1:1 ratio at a scanning range of 400-4000 cm^{-1} (PerkinElmer, Spectrum 2, USA) [17].

The FTIR spectra of Idronoxil combined with PCL were comparable to those of Idronoxil, showing that no chemical interactions between Idronoxil and PCL occurred under the conditions tested. In Figure 5, Idronoxil characteristic OH stretching vibration may be seen as a slight shoulder at 3424.46 cm^{-1} . Figure 6 show the FT-IR spectra of PCL polymer. The alcohol (OH stretching) vibration was recorded at 3421.53 cm^{-1} in the FTIR spectra of Idronoxil combined with PCL (Figure 7).

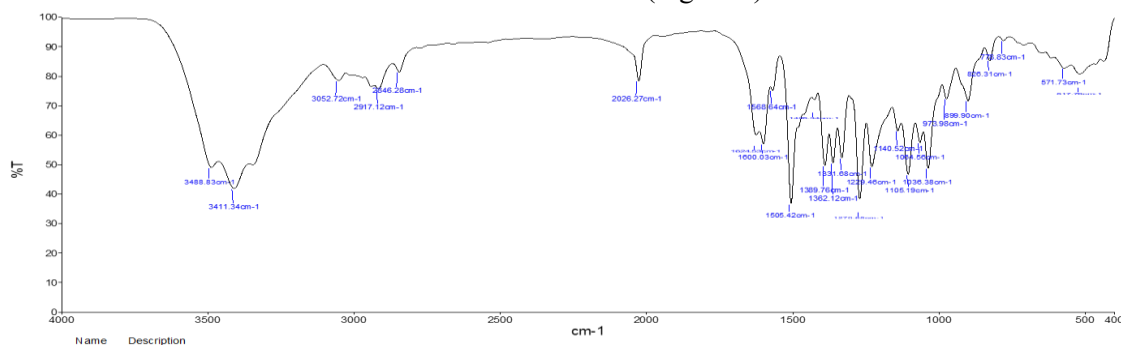


Figure 5. IR Spectrum of Idronoxil

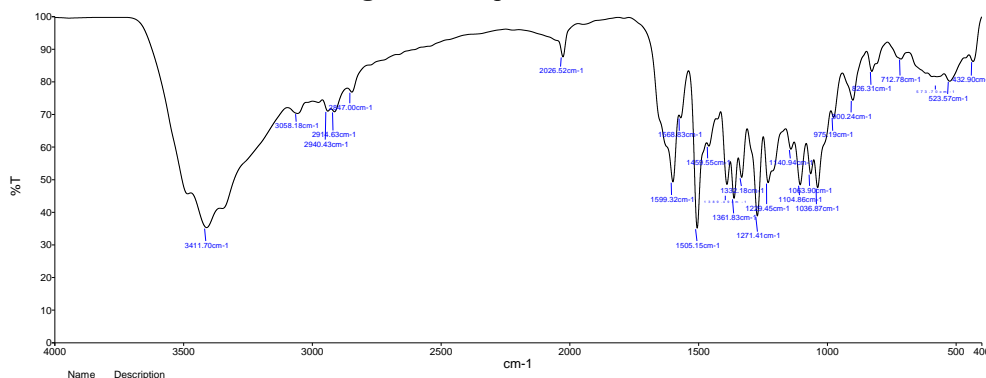


Figure 6. IR Spectrum of PCL

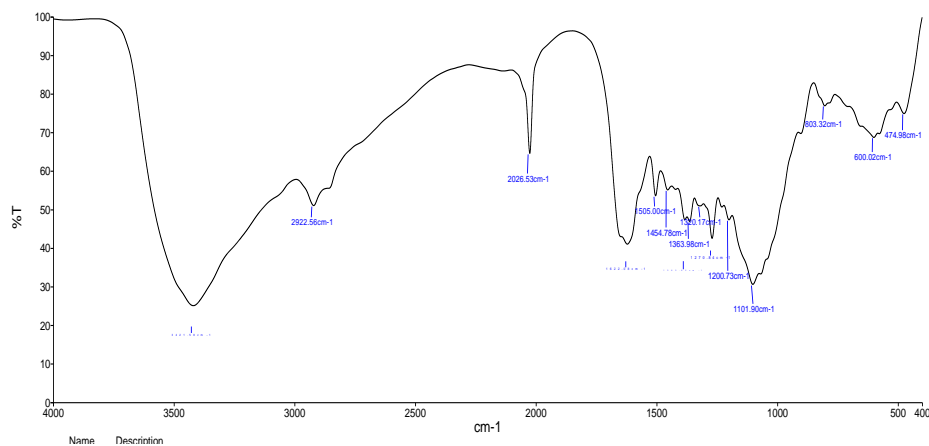


Figure 7. IR Spectrum of Idronoxil Loaded PCL Nanoparticles.

DSC Analysis

The DSC analysis was examining the drug's compatibility with the excipients. The calorimetry gives information on the biomolecule's stability, including its physical and chemical properties, as it analyses temperature and changes into nanoparticles temperature variation in the material's phase transition, As a result, the interplay between excipients and drug. The elimination of biomolecules can be used to conclude

development of new peaks at almost the same time. However, the appearance and geometry of the prior peaks are different. The peak in response to small changes in temperature, area, and enthalpy [18, 19].

For Idronoxil (figure 8) appearance of a sharp endothermic peak at 156°C was observed the fundamental endothermic peak at 166.89°C corresponding to its melting point, whereas PCL thermogram depicted a comparatively broad endothermic peak at 176°C (figure 9).

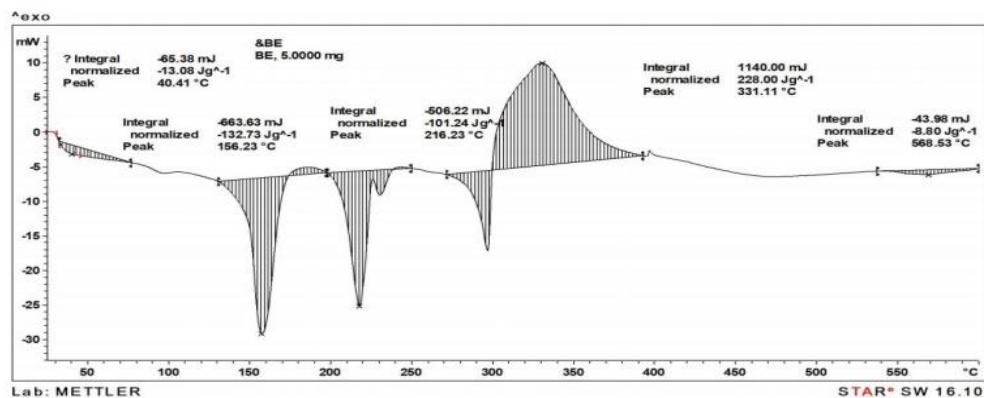


Figure 8. DSC Thermogram for Idronoxil

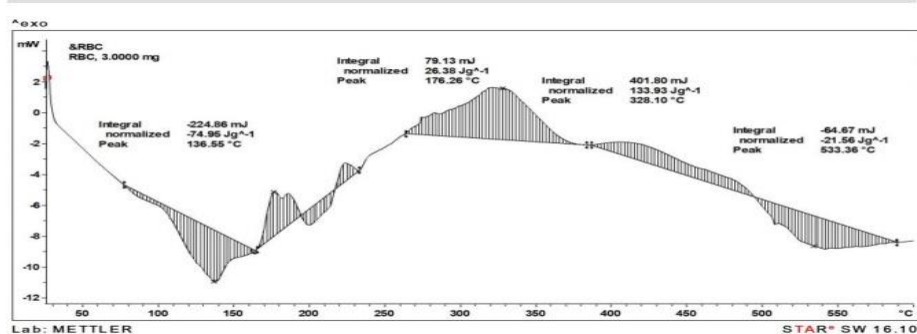


Figure 9. DSC Thermogram for Idronoxil PCL Nanoparticles

Characterization of Idronoxil Loaded PCL Nanoparticles

The SEM showed that the improved nanoparticles had a spherical form (Figure 10). The average particle size of nanoparticles was found to be 97.3 nm. The particle size distribution for improved Idronoxil-PCL-NPs

is shown in figure 11. Zeta and the polydispersity index potential were both determined to be at -6.41 mV in figure 12. The uniform particle dispersion and elevated physical stability of the delivery mechanism are evidenced by the low polydispersity index and the negative Zeta potential value [20].

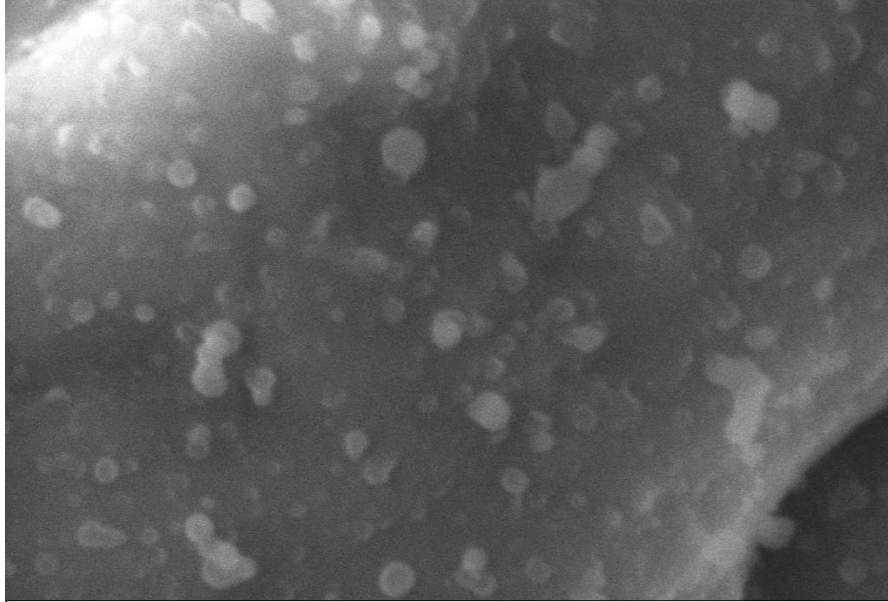


Figure 10. SEM Image of Idronoxil Loaded PCL Nanoparticles

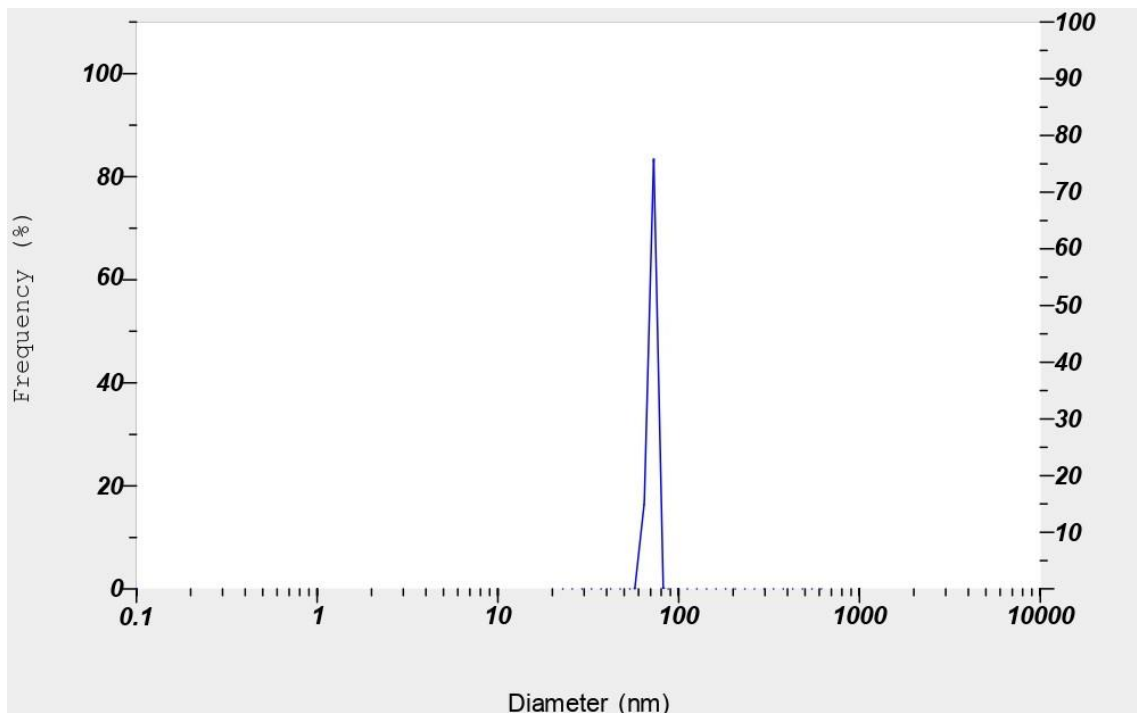


Figure 11. Dispersion of Particle Size of Idronoxil Loaded PCL Nanoparticles

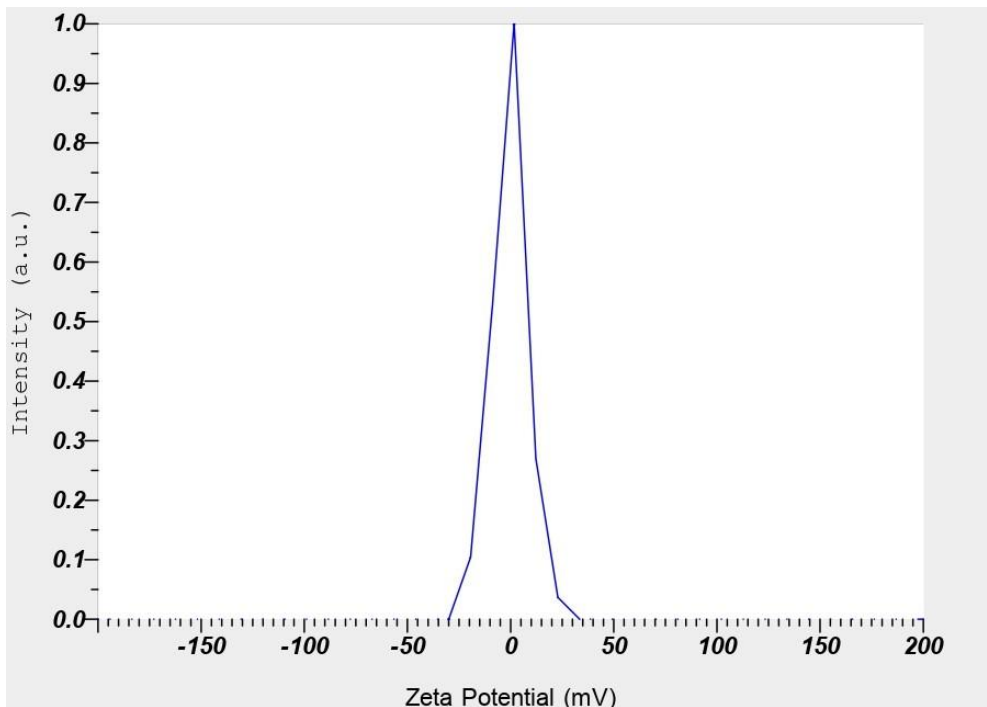


Figure 12. Zeta Potential of Idronoxil Loaded PCL Nanoparticles

Determination of Encapsulation Efficacy (EE)

The % EE has a significant impact on medication release as well as the overall efficacy of the manufacturing process. When PCL nanoparticles, has biocompatibility

properties, as well as excellent control of encapsulated substance release. Table 7 shows the encapsulation efficacy of Idronoxil. Figure 13 shows the Effect Idronoxil different concentrations of the encapsulation efficacy of PCL nanoparticles.

Table 7. Encapsulation Efficacy of Idronoxil

Compound	Area	Amt in S.Liquid	EE	% of EE
Idronoxil	266368.1	8.965	0.8207	82.07

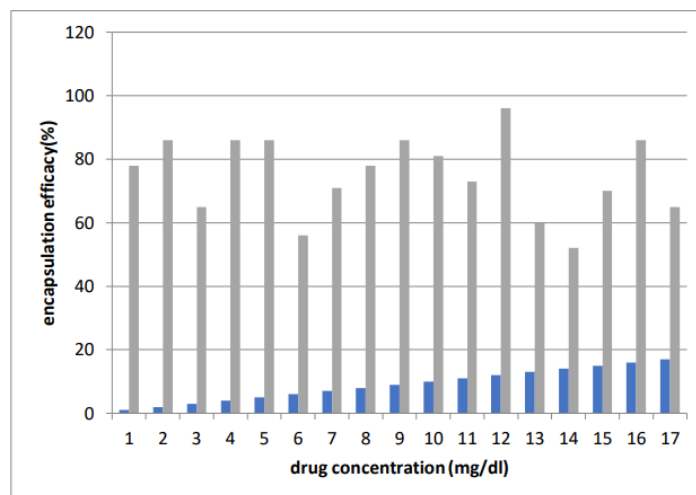


Figure 13. Effect Idronoxil Different Concentrations of the Encapsulation Efficacy of PCL Nanoparticles

In vitro Drug Release

Diffusion, erosion, and anaerobic decomposition of system delivery can all lead to drug release. Drug release from PCL

nanoparticles in phosphate buffer solution at pH 7.4, after 1 day of testing the in vitro drug release (figure 14). These PCL nanoparticles can release medications in a controlled manner, according to in-vitro release data.

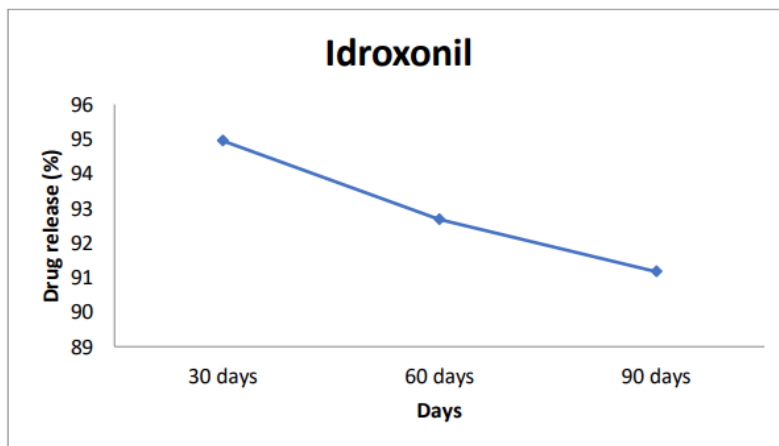


Figure 14. Idronoxil Loaded PCL Nanoparticles in *in-vitro* Drug Release Profile

Stability Testing

PCL nanoparticles were kept at room temperature for 90 days at 40°C±5°C. For 30-,

60- and 90-days nanoparticle samples were tested for drug release, uniformity drug content and any changes in their physical appearance (table 8 & figure 15).

Table 8. Stability Study Report on the Idronoxil

Evaluation parameter	30 days	60 days	90 days
Colour and appearance	No change	No change	No change
% drug content	98.64±1.5	97.98±1.06	96.58±1.68
% drug release	94.0. ±2.4	92.23±1.62	91.0±1.20

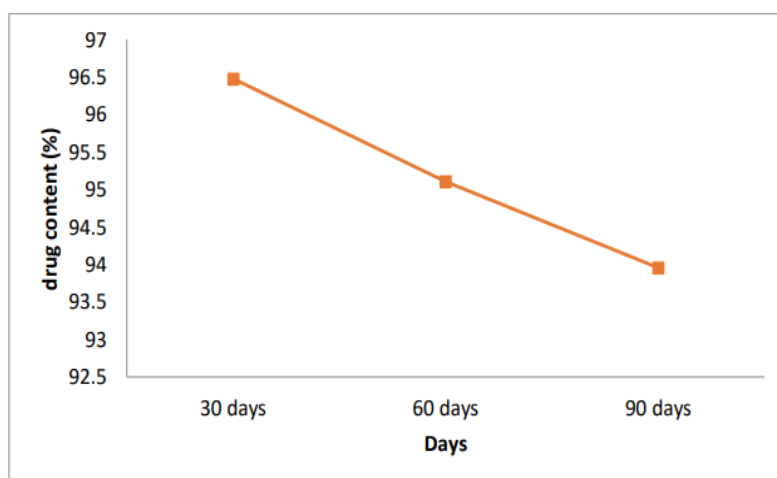


Figure 15. Stability Study Profile of Idronoxil Loaded PCL Nanoparticles

MTT Assay

MTT assay used to measure cell viability. Cell viability of synthesized chitosan nanoparticles was tested in HepG2 cell lines at various concentrations. At varying concentrations of 6.25, 12.5, 25, 50, and 100 μ g/ml, the synthesized nanoparticle showed Cell viability was reduced in a dose-

dependent manner, with a significant difference between the control and test groups. When the drug concentration was increased from 6.25 to 12.5 g/ml, cell diffusion improved as shown in figure 18. The IC50 value of the test samples for the production of Idronoxil PCL nanoparticles was 19.33 as shown in Table 9 & Figure 16.

Table 9. Cytotoxicity of Idronoxil Loaded PCL Nanoparticles on HepG2 Cell Line

SAMPLE	CONCENTRATION(μ g/ml)	VIABILITY(%)	IC50
Idronoxil loaded PCL nanoparticles	6.25	74.61	19.33
	12.5	59.46	
	25	40.77	
	50	32.71	
	100	15.63	

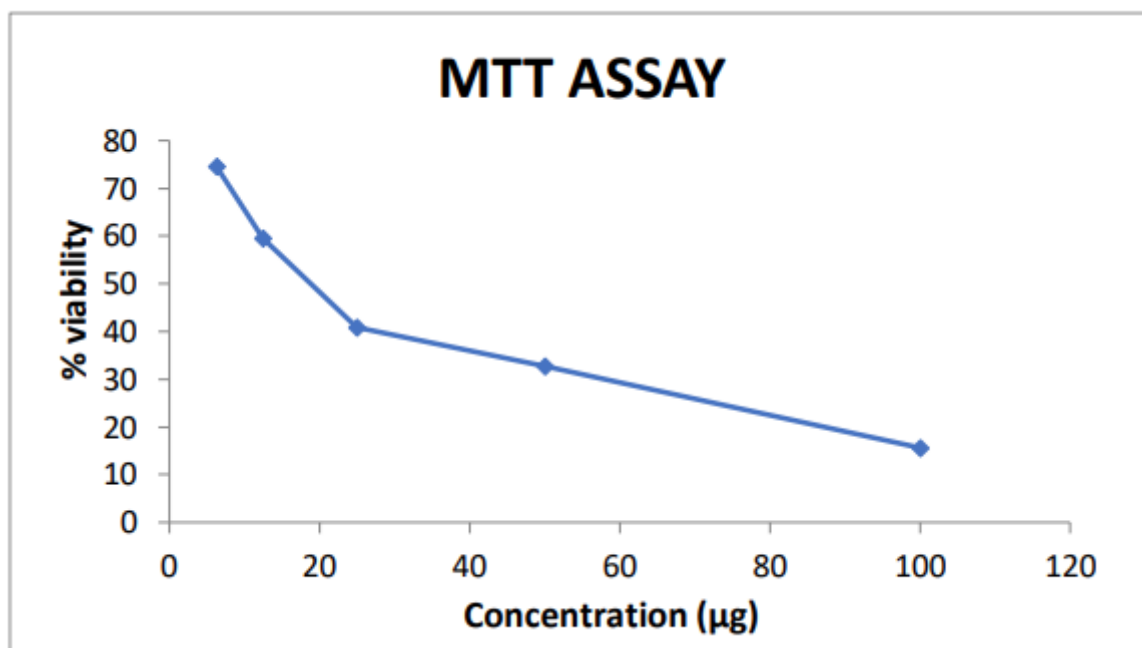


Figure 16. Graphical Representations of IC50 Values of Idronoxil Loaded PCL Nanoparticles on the HepG2 Cell Line in MTT Assay

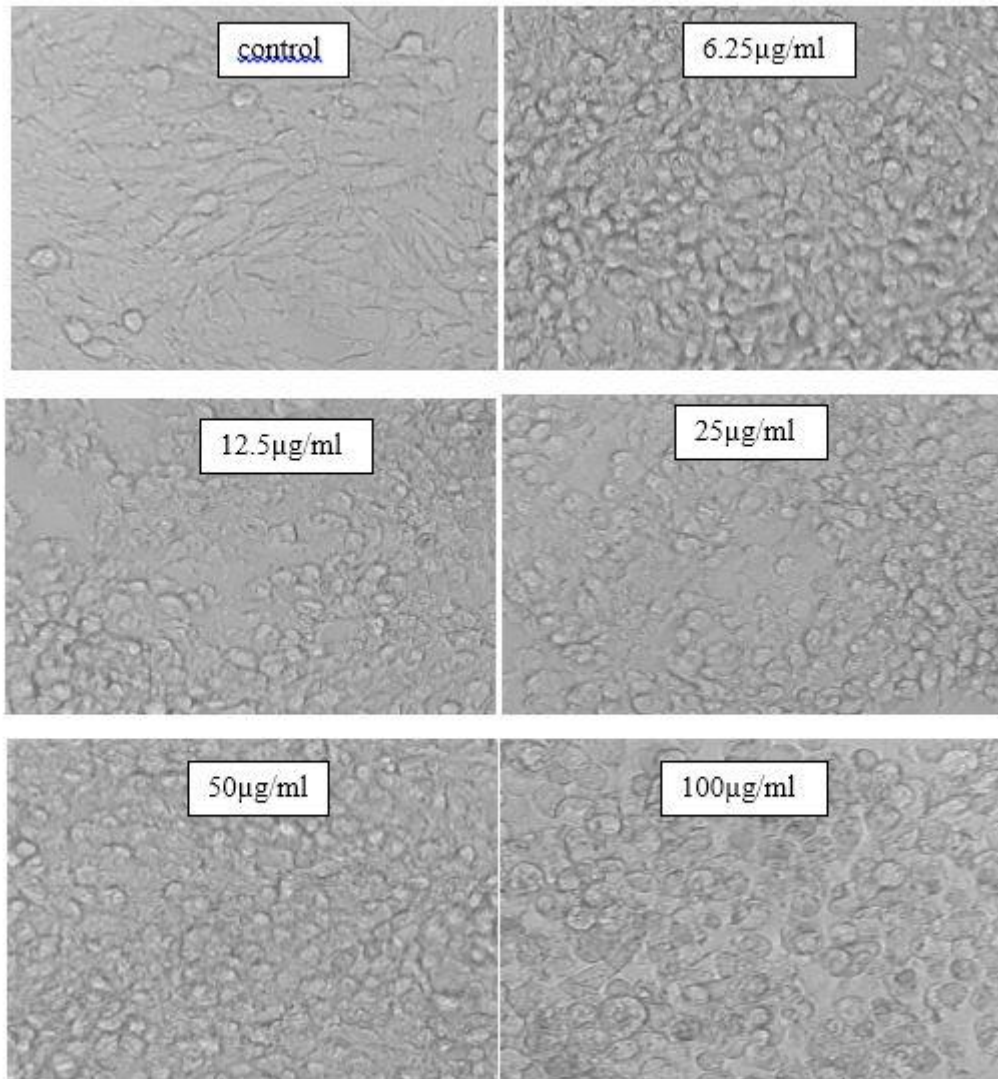


Figure 17. Images of HepG2 Cell Line at Varied Concentration of Idronoxil Loaded PCL Nanoparticles Treated Cells

Discussion

The present study successfully optimized and characterized Idronoxil-loaded polycaprolactone (PCL) nanoparticles using a factorial design approach. The ionic gelation method effectively produced stable nanoparticles with desirable particle size, zeta potential, and encapsulation efficiency. The quadratic models derived from the experimental data demonstrated a significant correlation between the independent variables PCL concentration, polyvinyl alcohol (PVA) concentration, and organic phase volume and the key quality attributes of the nanoparticles. The particle size of Idronoxil-PCL

nanoparticles ranged between 92 nm and 639 nm, significantly influenced by the concentrations of PCL and PVA. A higher PCL concentration led to an increase in particle size, which could be attributed to the enhanced viscosity and reduced dispersibility of the polymeric solution. Conversely, the surfactant (PVA) concentration demonstrated a biphasic effect; increasing PVA concentration initially reduced particle size due to improved stabilization of the emulsion droplets but caused aggregation and particle growth at excessive concentrations due to increased viscosity. These observations align with the findings of previous studies where surfactant

concentrations significantly impacted nanoparticle stabilization. The three-dimensional response surface plots revealed the intricate interplay of independent variables, highlighting their combined effects on particle size [21].

The zeta potential values, ranging from -2.4 mV to -13.7 mV, reflected the stability of the nanoparticles. A higher PCL concentration resulted in a more negative zeta potential due to the inherent anionic nature of PCL. Similarly, increased PVA concentration enhanced the negative charge on the nanoparticle surface, contributing to better colloidal stability. The ANOVA analysis indicated the significant contribution of organic phase volume to zeta potential, with higher volumes resulting in lower negative values. The observed trends are consistent with the electrostatic stabilization mechanism, where a higher absolute value of zeta potential ensures improved nanoparticle stability. The encapsulation efficiency of Idronoxil varied between 79% and 97.8%, with PCL concentration and organic phase volume being the most influential factors. Higher PCL concentrations enhanced the encapsulation efficiency due to increased polymer availability for drug entrapment. However, excessive polymer concentrations caused inefficient dispersion, leading to a decline in encapsulation efficiency. The interaction effects of PVA concentration and organic phase volume also played a critical role, as demonstrated by the response surface plots. These findings corroborate previous reports highlighting the critical balance of formulation parameters to achieve high encapsulation efficiencies. Using the desirability function approach, the optimized formulation was identified with minimal particle size, higher negative zeta potential, and maximum encapsulation efficiency. The experimental values closely matched the predicted outcomes, confirming the robustness and predictive accuracy of the optimization model. The overall desirability value of 0.939 underscores the effectiveness of

the optimization process in achieving the desired formulation attributes.

FT-IR spectroscopy confirmed the compatibility of Idronoxil with PCL, as no significant chemical interactions were observed. The characteristic peaks of Idronoxil remained intact in the physical mixture and nanoparticle formulations, indicating the stability of the drug within the polymer matrix. The characterization of Idronoxil-loaded PCL nanoparticles revealed essential insights into their morphology, size, stability, and encapsulation efficiency, demonstrating their potential as an effective drug delivery system. The SEM analysis confirmed that the nanoparticles were spherical, with a uniform size distribution and an average particle size of 97.3 nm. This nanoscale size is crucial for ensuring efficient cellular uptake and enhanced permeability. The zeta potential value of -6.41 mV, coupled with a low polydispersity index, indicates excellent colloidal stability and uniform dispersion of the nanoparticles, which are vital for maintaining their stability during storage and application [22]. The encapsulation efficiency (EE) of Idronoxil within PCL nanoparticles was recorded at 82.07%, as shown in Table 8. This high EE suggests effective drug incorporation, which is essential for reducing drug wastage and improving therapeutic outcomes. Figure 13 highlights that varying concentrations of Idronoxil affected the encapsulation efficiency, underscoring the importance of optimizing drug-to-polymer ratios for achieving the desired formulation characteristics. PCL, a biocompatible and biodegradable polymer, was instrumental in facilitating the sustained release of Idronoxil, enhancing its therapeutic potential [23, 24]. The *in vitro* drug release profile (Figure 14) demonstrated that the PCL nanoparticles provided a controlled and sustained release of Idronoxil in phosphate buffer solution (pH 7.4). This release mechanism, driven by diffusion, erosion, and biodegradation, ensures prolonged drug availability at the target site, potentially reducing dosing frequency and enhancing

patient compliance. Stability testing of the nanoparticles further validated their robustness. Over 90 days at 40°C±5°C, the nanoparticles maintained their physical appearance, drug content, and drug release profile, with minimal variations (Table 8 and Figure 15). This stability ensures the practical applicability of the formulation for long-term storage and usage [25].

Cytotoxicity studies using the MTT assay confirmed the anticancer potential of Idronoxil-loaded PCL nanoparticles against HepG2 liver cancer cells. The nanoparticles exhibited a dose-dependent reduction in cell viability, with an IC₅₀ value of 19.33 µg/mL, as shown in Table 9 and Figure 17. This significant cytotoxic activity highlights the potential of these nanoparticles as an effective therapeutic agent for liver cancer. The dose-dependent nature of the cytotoxic effect indicates that higher concentrations of the nanoparticles were more effective in inducing cell death, which is evident from the improved diffusion and cellular uptake at higher drug concentrations (Figure 17) [26]. Overall, the results emphasize that Idronoxil-loaded PCL nanoparticles are a promising drug delivery system due to their excellent stability, controlled release properties, and potent anticancer activity. Future studies focusing on in vivo efficacy and detailed mechanistic investigations could further validate their clinical utility.

Conclusion

The present study successfully optimized and characterized Idronoxil-loaded polycaprolactone (PCL) nanoparticles, demonstrating their potential as a robust and effective drug delivery system. The application of a factorial design approach enabled the identification of optimal formulation parameters, achieving desirable particle size, high encapsulation efficiency, and excellent colloidal stability. The nanoparticles exhibited a spherical morphology with a nanoscale size suitable for enhanced cellular uptake and

permeability, as well as a negative zeta potential that ensured stability and uniform dispersion. The sustained and controlled drug release profile, combined with robust stability under accelerated conditions, highlighted the suitability of these nanoparticles for long-term therapeutic applications.

Furthermore, cytotoxicity studies revealed significant dose-dependent anticancer activity against HepG2 liver cancer cells, confirming the therapeutic potential of Idronoxil-loaded PCL nanoparticles. The findings of this study underscore the importance of optimizing formulation parameters to achieve an efficient and stable drug delivery system. These nanoparticles offer a promising platform for targeted and sustained drug delivery in cancer therapy. Future research should focus on in vivo studies and clinical trials to further establish their efficacy and safety in real-world applications.

Author Contributions

Lokeshvar Ravikumar: Conceptualization, Methodology, Investigation, Data Curation, Formal Analysis, Writing—Original Draft, and Project Execution. Ramaiyan Velmurugan: Supervision, Project Administration, Study Design, Writing—Review & Editing, and Final Approval of the Manuscript. Vinod Kumar Teriveedhi: Data Analysis, Validation, and Writing—Review & Editing. Pradeep Vidiyala: Software and Statistical Analysis. Patibandla Jahnvi: Experimental Work and Data Collection. Rajeshwar Vodeti: Literature Review and References Management. Selvaraja Elumalai: Resources and Writing—Review & Editing.

Conflict of Interest

The authors hereby declare that there is no conflict of interest in this study.

Acknowledgement

Authors would like to thank Saveetha College of Pharmacy, Saveetha Institute of Medical and Technical Sciences, Chennai, India

for providing research facilities to carry out this work.

References

- [1]. Volk, M. L., Marrero, J. A., 2008, Early detection of liver cancer: Diagnosis and management, *Current Gastroenterology Reports*, 10(1), 60-6.
- [2]. Tsai, W. C., Kung, P. T., Wang, Y. H., Kuo, W. Y., Li, Y. H., 2018, Influence of the time interval from diagnosis to treatment on survival for early-stage liver cancer, *PLoS ONE*, 13(6), e0199532.
- [3]. Paramasivam, G., Sanmugam, A., Palem, V. V., Sevanan, M., Sairam, A. B., Nachiappan, N., Youn, B., Lee, J. S., Nallal, M., Park, K. H., 2024, Nanomaterials for detection of biomolecules and delivering therapeutic agents in theragnosis: A review, *International Journal of Biological Macromolecules*, 254, 127904.
- [4]. Barabadi, H., Mostafavi, E., Saravanan, M. (Eds.), 2022, *Pharmaceutical Nanobiotechnology for Targeted Therapy*, Springer International Publishing AG.
- [5]. Mir, S. A., Dar, A., Hamid, L., Nisar, N., Malik, J. A., Ali, T., Bader, G. N., 2023, Flavonoids as promising molecules in cancer therapy: An insight, *Current Research in Pharmacology and Drug Discovery*, 100167.
- [6]. Porter, K., Fairlie, W. D., Laczka, O., Delebecque, F., Wilkinson, J., 2020, Idronoxil as an anticancer agent: Activity and mechanisms, *Current Cancer Drug Targets*, 20(5), 341-54.
- [7]. Bhadrans, A., Shah, T., Babanyinah, G. K., Polara, H., Taslimy, S., Biewer, M. C., Stefan, M. C., 2023, Recent advances in polycaprolactones for anticancer drug delivery, *Pharmaceutics*, 15(7), 1977.
- [8]. Bhardwaj, H., Jangde, R. K., 2023, Current updated review on preparation of polymeric nanoparticles for drug delivery and biomedical applications, *Next Nanotechnology*, 2, 100013.
- [9]. Rohatgi, N., Ganapathy, D., Sathishkumar, P., 2023, Eradication of *Pseudomonas aeruginosa* biofilm using quercetin-mediated copper oxide nanoparticles incorporated in the electrospun polycaprolactone nanofibrous scaffold, *Microbial Pathogenesis*, 185, 106453.
- [10]. Pedroso-Santana, S., Fleitas-Salazar, N., 2020, Ionotropic gelation method in the synthesis of nanoparticles/microparticles for biomedical purposes, *Polymer International*, 69(5), 443-7.
- [11]. Haroosh, H. J., Dong, Y., Jasim, S., Ramakrishna, S., 2021, Improvement of drug release and compatibility between hydrophilic drugs and hydrophobic nanofibrous composites, *Materials*, 14(18), 5344.
- [12]. Alkammash, N. M., 2017, Synthesis of silver nanoparticles from *Artemisia Sieberi* and *Calotropis Procera* medical plant extracts and their characterization using SEM analysis, *Biosciences Biotechnology Research Asia*, 14(2), 521-6.
- [13]. Reddy, Y. P., Chandrasekhar, K. B., Sadiq, M. J., 2015, A study of *Nigella sativa* induced growth inhibition of MCF and HepG2 cell lines: An anti-neoplastic study along with its mechanism of action, *Pharmacognosy Research*, 7(2), 193.
- [14]. Ghasemi, M., Turnbull, T., Sebastian, S., Kempson, I., 2021, The MTT assay: Utility, limitations, pitfalls, and interpretation in bulk and single-cell analysis, *International Journal of Molecular Sciences*, 22(23), 12827.
- [15]. Nga, N. T., Ngoc, T. T., Trinh, N. T., Thuoc, T. L., Thao, D. T., 2020, Optimization and application of MTT assay in determining density of suspension cells, *Analytical Biochemistry*, 610, 113937.
- [16]. Kessaissia, F. Z., Zegaoui, A., Aillerie, M., Arab, M., Boutoubat, M., Fares, C., 2020, Factorial design and response surface optimization for modeling photovoltaic module parameters, *Energy Reports*, 6, 299-309.
- [17]. Tkachenko, Y., Niedzielski, P., 2022, FTIR as a method for qualitative assessment of solid samples in geochemical research: A review, *Molecules*, 27(24), 8846.
- [18]. Budiman, A., Handini, A. L., Muslimah, M. N., Nurani, N. V., Laelasari, E., Kurniawansyah, I. S., Aulifa, D. L., 2023, Amorphous solid dispersion

as drug delivery vehicles in cancer, *Polymers*, 15(16), 3380.

[19]. Qiu, X. L., Fan, Z. R., Liu, Y. Y., Wang, D. F., Wang, S. X., Li, C. X., 2021, Preparation and evaluation of a self-nanoemulsifying drug delivery system loaded with heparin phospholipid complex, *International Journal of Molecular Sciences*, 22(8), 4077.

[20]. Danaei, M. R., Dehghankhold, M., Ataei, S., Hasanzadeh Davarani, F., Javanmard, R., Dokhani, A., Khorasani, S., Mozafari, M. R., 2018, Impact of particle size and polydispersity index on the clinical applications of lipidic nanocarrier systems, *Pharmaceutics*, 10(2), 57.

[21]. Agrawal, M., Saraf, S., Pradhan, M., Patel, R. J., Singhvi, G., Alexander, A., 2021, Design and optimization of curcumin-loaded nano lipid carrier system using Box-Behnken design, *Biomedicine & Pharmacotherapy*, 141, 111919.

[22]. Tantra, R., Schulze, P., Quincey, P., 2010, Effect of nanoparticle concentration on zeta-

potential measurement results and reproducibility, *Particuology*, 8(3), 279-85.

[23]. Mohamed, R. M., Yusoh, K., 2016, A review on the recent research of polycaprolactone (PCL), *Advanced Materials Research*, 1134, 249-55.

[24]. Mehmood, A., Raina, N., Phakeenuya, V., Wonganu, B., Cheenkachorn, K., 2023, The current status and market trend of polylactic acid as biopolymer: Awareness and needs for sustainable development, *Materials Today: Proceedings*, 72, 3049-55.

[25]. Bai, X., Smith, Z. L., Wang, Y., Butterworth, S., Tirella, A., 2022, Sustained drug release from smart nanoparticles in cancer therapy: A comprehensive review, *Micromachines*, 13(10), 1623.

[26]. Augustine, R., Hasan, A., Primavera, R., Wilson, R. J., Thakor, A. S., Kevadiya, B. D., 2020, Cellular uptake and retention of nanoparticles: Insights on particle properties and interaction with cellular components, *Materials Today Communications*, 25, 101692.